SHAFT DESIGN PROJECT REPORT

Snowmobile sub-assembly design exercise

Rebecca Heidenreich (rh2095) & Cris Dignadice (cd927)

University of Bath | ME20014

Shaft Design Project Report

Snowmobile sub-assembly design exercise

Summary

Macaulay's notation was applied to the free-body diagrams of the initial design concepts to analyse the magnitude of loading at certain locations on the shaft. Pugsley's Method was used to calculate the design factor of the shaft, which affected the allowable stress. The combined stresses at each concentration area were then compared to the allowable stress, producing a percentage. This percentage aided in optimising diameters to allow for the fittings of standard components. To transmit torque from the motor shaft to the drive shaft, synchronous pulleys and a belt drive were selected. Deep groove ball bearings were chosen due to cost and proficient load bearing. Keys were used to transmit torque onto the track sprockets and driven pulleys which were located using taper lock bushes, shoulders, sleeves, and circlips.

Introduction

This project aimed to re-design a detailed rear axle sub-assembly for a snowmobile. This included the shaft and its supporting components. It needed to support the load and transmit power to the tracks. The key factors to consider for the re-design were to make the design easier and cheaper to manufacture and assemble; to avoid embedded carbon in the materials; and to make it as lightweight as possible to reduce fuel consumption. Our design approach was to follow all requirements whilst optimising our shaft as much as possible to reduce embedded carbon and weight, ensuring efficiency not only in operation but also in manufacturing. Parallel to this was making sure the stresses were minimised and trying to create a design which was cost-effective and suitable for small-batch production.

Initial Analysis

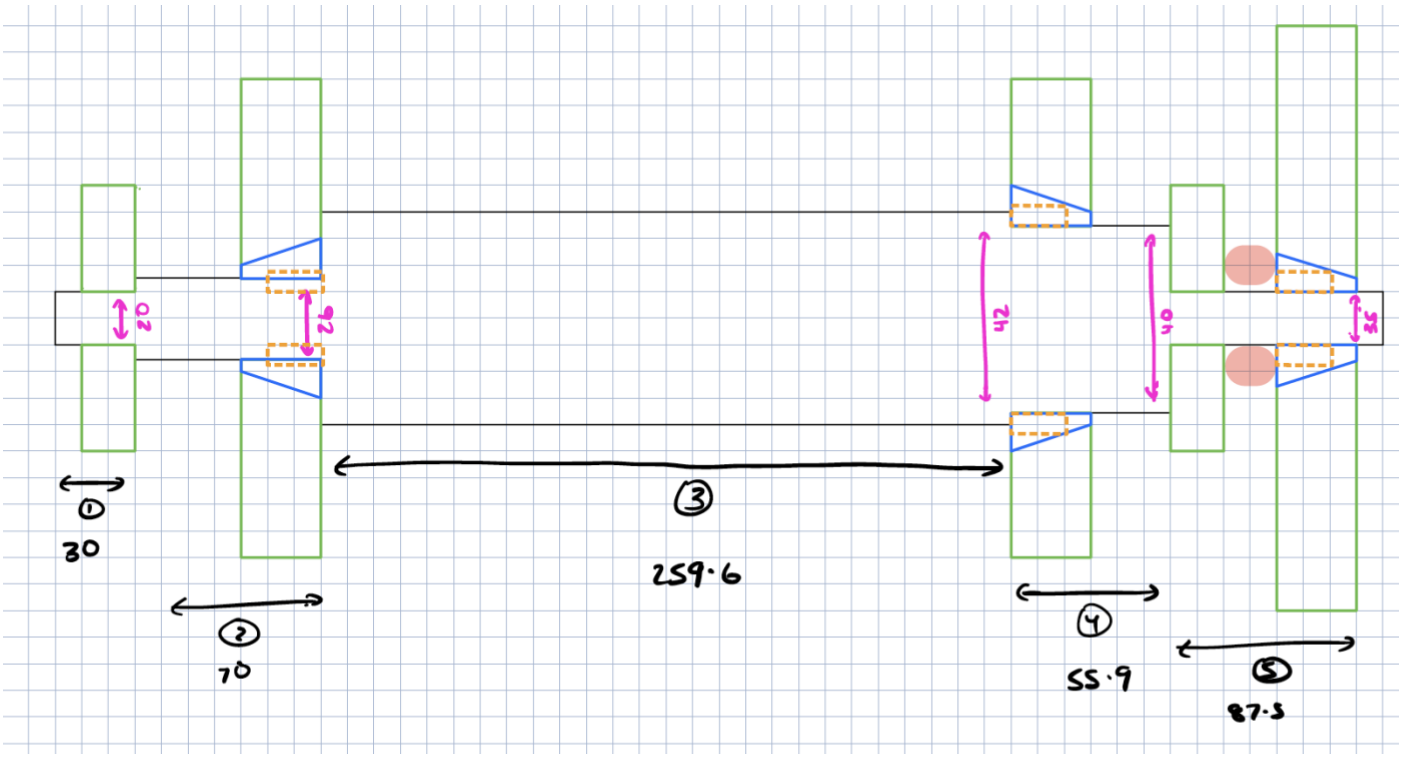

Figure 1: Initial Design Concept

Forces on Inside Sprocket

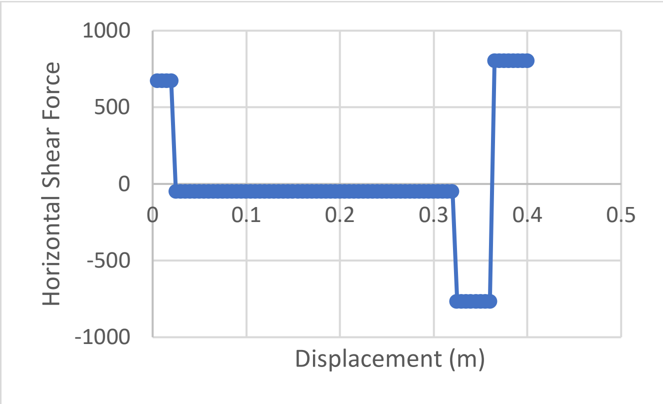

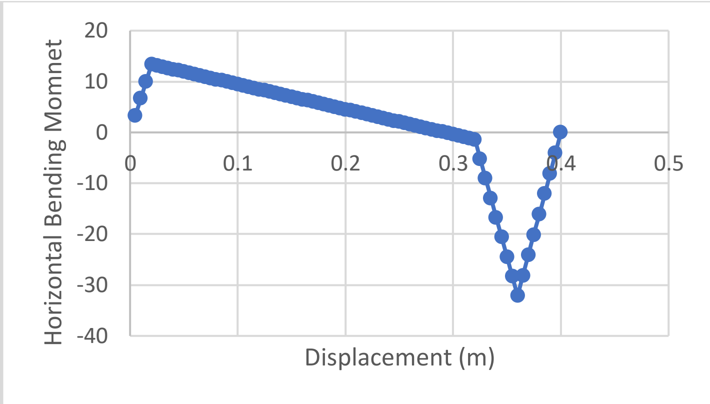

Figure 2: Horizontal Shear Force Diagram

Figure 3: Horizontal Bending Moment diagram

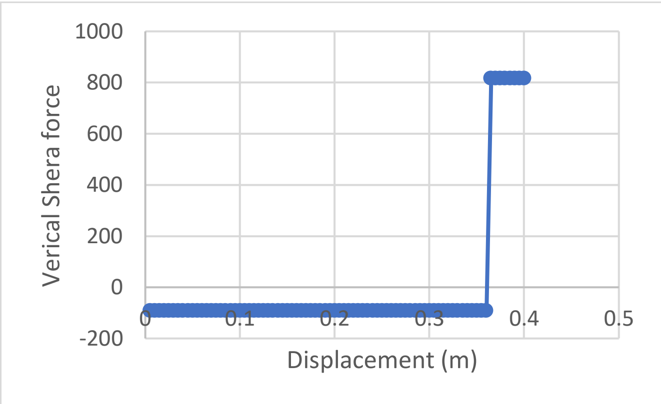

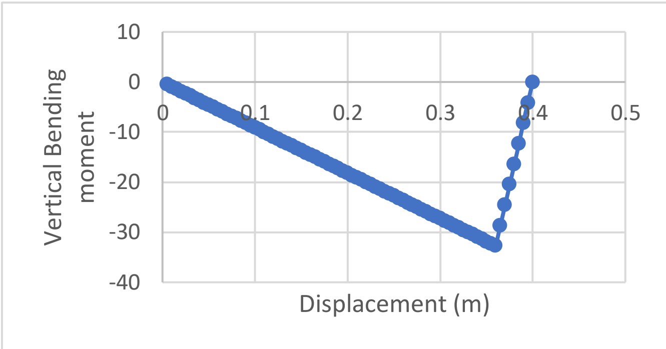

Figure 4: Vertical Shear Force Diagram

Figure 5: Vertical Bending Moment Diagram

Forces on Outside Sprocket

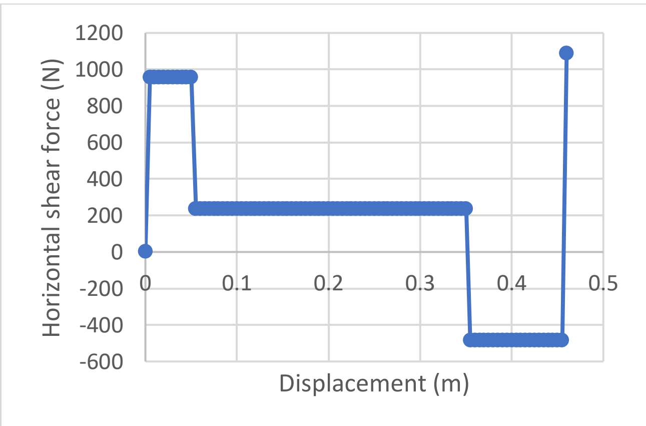

Figure 6: Horizontal shear force diagram

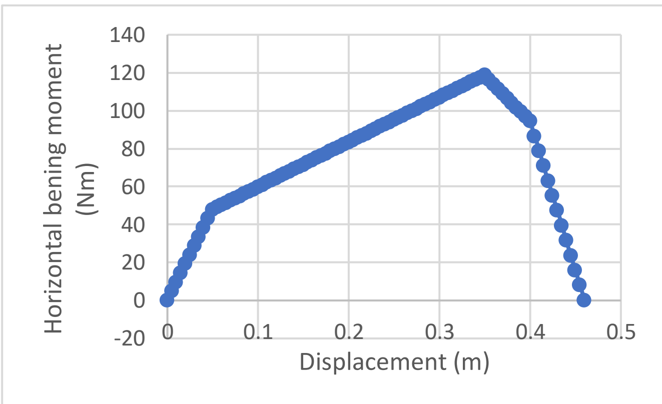

Figure 7: Horizontal bending moment diagram

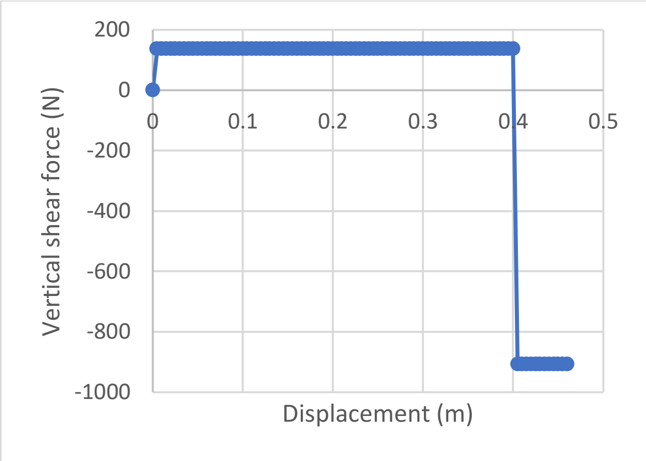

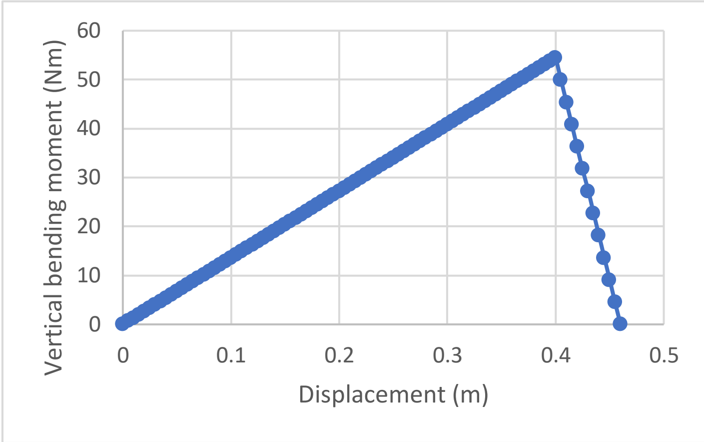

Figure 8: Vertical shear force diagram

Figure 9: Vertical bending moment diagram

Design Options

Design Factor

There are multiple sources of uncertainty, for example, shocks, fatigue, and material properties. To account for this a design factor is used. The design factor reduces the allowable stress to account for any uncertainty and other effects and is a ratio of nominal strength to allowable stress.

$$\sqrt{\sigma^2 + 3\tau^2} \geq \frac{S_Y}{N_Y}$$

Where N_Y = design factor for yield = bcd
Where b = fatigue factor
c = shock factor
d = safety factor

In this design we identified:

- that the stress on the component would vary between tension and compression, so b = 1.5.
- loads would suddenly be applied, so c = 2.

For safety factors, Pugsley's method was applied, which splits d into two factors.

$$d = XY$$

X reflects the probability of failure which relates to:
A – materials, workmanship, inspection, and manufacture
B – loading, considering the level of control over the use
C – the quality of assessment of strength and analysis methods

For A, we decided all the factors were going to be of a high standard, so very good, VG, was selected.
For B, we discussed that our level of control over the use of the snowmobile was very poor, as someone completely inexperienced or irresponsible could be in possession of it.
For C, we decided that we were doing a high-quality assessment, so very good was chosen.
Table 1 in Appendix 1 was followed and an X factor of 1.7 was reached.

Y reflects the seriousness of failure which relates to:
D – danger to people
E – economic consequences

For D – if the snowmobile were to fail, the user could die, so a very serious factor
For E – if this were to break, there is little impact on the economy and would probably not have a huge impact on the company's sales so it's not a serious design factor. Following table 2 in appendix 1, a Y-factor of 1.4 was selected.
This gave a final design factor of 6.12.

Comparing stress and allowable stress

For the final design, we decided to go with EN24, a medium carbon low alloy steel with a yield strength of 680MPa and a density similar to the others of $7900kgm^{-3}$. Despite EN24 having the higher embodied carbon per kg, it provided the largest allowable stress for our chosen design factor, leading to reduced diameters, and therefore mass, of the final shaft. The changes made to the shaft geometry were based on the ratio between the combined stress of the bending and torsional load at the local area, the allowable stress provided by the material and the key loading constraints. In addition to this, nodes 2 and 4 were constrained to diameters that were a multiple of 5 due to the standard components produced by the manufacturers.

In response to the client's first question, looking at the shaft only from a loading point of view, the sprocket inside the bearing would prove to be the better choice. It shortened the shaft due to the 400mm between bearings constraint and reduced the loads drastically. At nodes 2, 3 and 4 with the sprocket being situated inside the bearing, the combined stress values were 51.9MPa, 33.2MPa and 26.4MPa respectively compared to the sprocket outsides values of 89.9MPa, 35.3MPa and 39.7MPa. This translates to a decrement of 27.3% on average across the 3 investigated nodes. Regardless, this isn't the design we opted for. Placing the sprocket on the inside of the bearing produces challenges with maintenance regarding the shaft. In the scenario that the chain/belt being used is broken, the user must remove the shaft from the bearing housing, essentially removing the whole drive shaft assembly from where it's situated. Meanwhile, if this were the case with the sprocket being outside the bearing, this problem could be solved without moving the entire shaft. Additionally, the bearings being further away from the main power source means that, theoretically, the reaction forces produced from the bearings are larger due to the larger distances.

The ratio between the combined stresses and allowable stress was looked at in the form of a percentage. If the percentage was below 100%, the force stayed within the range that we can safely operate at. With the diameters chosen, the highest percentage was 80.9% for the shaft, with the calculations for the key coming close behind at 78.6%. As seen in the shear force and bending moment diagrams above, the sections experiencing the largest forces were node 4 and node 5 meaning that presumably these nodes would be the thickest. The diameter of the shaft was partly constrained due to the force acting locally onto the key being dependent on the local node diameter. A lower shaft diameter transfers more torque onto the keys due to the equation:

$$F = \frac{Q}{r}$$

Therefore, it was important to make sure that the shaft ratios stayed under 100%, but even more so important to not forget that changing diameter values would impact the forces the keys experienced.

To calculate the effective load acting on the key, the following equation was used:

$$\sigma_{eff} = \frac{32}{\pi d^3}\sqrt{(K_b M)^2 + \frac{3}{4}(K_t T)^2}$$

The effective load is used in durability calculations, accounting for the maximum and minimum loads. This particular equation only accounts for the torsional and bending forces. The effective load was then compared to the yield stress of the key material, a similar operation to the shaft. With the percentages staying under well 100%, we were able to safely conclude that the keys wouldn't break or shear under the forces and moved onto optimisation.

Note: the calculations for the loadings for the case the sprocket was inside the bearing can be found in Appendix 2.

Transmission selection

For transmission, a chain or belt drive could have been selected. Chain drives have a low initial cost, do not deteriorate from outdoor use, and can operate in wet conditions, they are easy to manufacture and assemble and valuably, can be fixed without having to take apart the whole assembly. However, they stretch and have associated maintenance costs. Belt drives are a higher initial cost, however, have no running costs. They are lower maintenance and do not stretch, however, are more hassle to repair as once broken they must be replaced, which requires deconstruction. They also have higher efficiency and experience less wear. With this information we initially chose a chain drive, however, we could not find a suitable Fenner chain (calculations in Appendix 3) and the Renolds chain was only just allowable and was there to be any design changes or remodelling of the snowmobile, the chain selection would have to be revisited. Subsequently, a Fenner synchronous belt was selected, answering the client's second question that a belt drive *would* improve the design.

Bearing selection

There were many design changes made to the bearing choice. In the end, 6204-RSH and 6008-2RS1 were chosen. Both of these bearings are Deep groove ball bearings (DGBB), providing a good mix between low friction, low noise, and low vibration. DGBB can accommodate radial and axial loads in both directions and require less maintenance compared to other bearings. These bearings also come with seals, providing a way to stop contamination and lubrication leakage.

A bearing that was considered was SKF's Compact Aligning Roller Bearing (CARB). The bearing is ably accommodating to linear expansion due to thermal differentials, misalignment, and heavy loads. However, these bearings didn't come with a sealing option for our diameter, leading to us having to include some sort of sealing mechanism. We decided that this wasn't worth the effort as CARB bearings are also much more expensive than DGBBs and were essentially overkill in the first place.

When a radial load is applied to the bearing, the inner ring will expand slightly resulting in the bore expanding minutely. Due to this, the initial interference is reduced. In the case that the force is, F, is smaller than or equal to 0.25C_0, then the reduction of the interference can be calculated as follows:

$$d_1 = \sqrt{0.08(\frac{Fd}{B})}$$

In the case that F is larger than 0.25C_0, then we use the following:

$$d_1 = 0.02(\frac{F}{B})$$

Where:
d_1 = reduction of inner ring interference (mm), d = nominal bore diameter of bearing, B = nominal inner ring width, F = radial load, C_0 = basic static load rating

For our bearings, this resulted in a diameter reduction of $1.38 \times 10^{-3} mm$ in the 6204-RSH bearing and $1.29 \times 10^{-3} mm$ for the 6008-2RS1 bearing.

Additionally, when the inner ring operates under a load, the temperature generally becomes higher than that of the shaft resulting in the effective interference decreasing due to the greater thermal expansion of the inner ring.

Assuming the temperature difference between the bearing house and the surrounding housing is dt, then the temperature difference at the fitting surfaces of the inner ring and shaft will approximately be (0.10~0.15) x dt.

The reduction in interference, d_1, is then expressed as follows:

$$d_1 = (0.10{\sim}0.15)dt\alpha d$$

The reduction of the inner ring interference of 6204-RSH due to temp is $3.4375 \times 10^{-4} mm$ and $6.875 \times 10^{-4} mm$ for 6008-2RS1.

Table 1: thermal expansion of shaft calculations

Thermal expansion of shaft
0.004527
dL = LαdT
dT = 75

Table 2: comparative table for load ratings with different bearings

Position	**Basic dynamic load rating (Ball bearing) (kN)**	**Basic dynamic load rating (Roller bearing) (kN)**	**Static load value (kN)**
A	2.022927149	0.980543967	1.448266661

B	3.159669603	1.531540554	2.26209043

Shaft fixtures and fittings

The use of splines and keys was discussed to transfer torque from the driven pulley to the shaft. Although a spline is more efficient in terms of transferred power, it is more expensive thus making it unsuitable for small-batch production. With this conclusion, we opted to use taper lock bushes and keys for location along with a circlip and shaft sleeve. For nodes 2 and 5, where there are sprockets transmitting torque, 1210-26, 2012-40 and 2012-35 taper lock bushes were used respectively. The use of taper lock bushes was chosen due to the way it inherently locates onto a shaft. Due to this, we were able to reduce the overall number of shoulders in the design and could avoid using circlips, which produced an extremely high-stress concentration, along the highly loaded sections of the shaft.

To locate the bearing at section 1 (6204-RSH), a circlip was used. We were able to do this due to the circlip being positioned outwards of the bearing, resulting in there not being any forces in the local area. The circlip prohibits axial movement of the bearing but will expand with the shaft due to thermal expansion or contraction. Assuming that the average ambient temperature is 15 degrees, the shaft would thermally expand $2.15 \times 10^{-7} mm$ and contract $2.46 \times 10^{-7} mm$. These values are extremely small, almost negligible. Despite this, a float of 0.5mm was added. The values will also be considered when choosing tolerances.

To locate the bearing at section 5 (6008-2RS1), it was rested up against the shoulder and was kept axially in place by the SPEEDI SLEEVE used. Initially, we decided against using a sleeve and opted for another shoulder or a circlip for location due to the specification stating to minimise sliding of tight tolerances parts over each other. Using a circlip increased the diameter to a minimum of 37.5mm, which would have needed to be rounded to 40mm due to standard bearings only coming in bore diameters of 5mm. The sleeve was used to avoid the need of creating another shoulder, resulting in another local stress concentration, and to reduce the diameter as much as possible.

The keys were given a close/interference fit of p9 tolerance, ensuring that the key and keyway were fitted snugly reducing the amount of lateral play and maximising torque transmission. The shafts with taper lock bushes were tolerances at h6, as per the recommendation of *PTI Taper Bushes*. To ensure that the nodes over which the bearings slide have the correct circularity, the drawings included circular and total runoffs. The bearing tolerance, as per *SKF*, was stated to be p6**.** A p6 tolerance equates to an international tolerance grade of IT5. This gave us a circular runout value of $3\mu m$. As such, the total runout was made to also be $3\mu m$, ensuring the entire node length was as close to being the required diameter, with respect to the datum, as possible.

Final Design

Loading tolerance for Final design

Table 3: Final loading calculations for final design - sprocket on the outside

Node	**1**	**2**	**3**	**4**	**5**
Diameter, d (m)	0.02	0.026	0.042	0.04	0.035
J value	1.5708E-08	4.48635E-08	3.0549E-07	2.51327E-07	1.47324E-07
I value	7.85398E-09	2.24318E-08	1.52745E-07	1.25664E-07	7.36618E-08
Vertical BM	0	47.973	118.551	94.344	0
Horizontal BM	0	0	0	54.4696	0
Combined BM	0	47.973	118.551	108.9391007	0
Torque	0	-104.4	-104.4		208.8
Bending SCF	1.699037007	1.740394715	1.853121401	2.288077839	1.879418825
Torsional SCF	1.49627285	1.445963885	1.473020046	1.369761645	1.795410245
Nominal Bending stress	0	27802057.66	16298868.51	17338196.37	0
Max bending stress	0	48386554.21	30203782.05	39671142.89	0

Nominal Torsional stress	0	-30251754.32	-7176666.044	0	24802557.85
Max torsional stress	0	-43742944.2	-10571372.95	0	44530766.46
Combined stresses	0	89897687.02	35320393.94	39671142.89	77129550.01
Allowable stress	111111111.1	111111111.1	111111111.1	111111111.1	111111111.1
OK?	0	80.90791831	31.78835454	35.7040286	69.41659501
Volume	9.42478E-06	3.7165E-05	0.000359661	7.0246E-05	8.41849E-05
Mass	0.074455746	0.293603825	2.84132061	0.554943493	0.665060439

Table 4: Weight and cost summary

Total mass (Kg)	4.413
Carbon usage (Kg)	11.56
Cost of final shaft (£)	11.74
Initial cost of billet (£)	14.64

Transmission

The Fenner Synchronous Belt drive selection guide was followed:

Drive requirements
- 10 hours per week, 10 years
- Driving speed: 3000 rpm, Driven speed: 916 rpm
- Power: 20kW motor
- Required centre distance: 415-450mm

1. Design power = service factor x running power = 1.5 x 20 = 30kW
   - Service Factor: soft start, 10 and under hours per day, heavy duty = 1.5
2. Belt pitch: 8mm
3. Speed ratio = 3.275
4. A speed ratio of 3.29 satisfied a +/- 2% criterion and satisfied the centre distance requirements. This gave a driving pulley groove number of 34 and the driven 112, the centre distance 416mm.
5. Using 416mm centre distance, belt length pitch = 1440 mm

6.1. Power rating = 19.66 kW
6.2. Belt length corrected power rating = power rating x belt length correction factor = 19.66 x 1.1 = 21.626 kW
6.3. Belt width factor = $\frac{design\ power}{\text{Belt length corrected power rating}} = \frac{30}{21.626} = 1.387$

6.4. Step 7.3 gives belt width of 30mm, for a width factor of 1.58 which is greater to or equal to 1.387.

7. Drive specification
   Motor pulley: 34-8M-30 HTD pulley
   Driven pulley: 112-8M-30 HTD pulley
   Taper lock bush: 2012/35 mm
   Belt: 8 MXP Fenner Torque Drive Plus 3 Belt

Note: tables used for reference in this section can be found in appendix 3.

Bearings

Table 5: Final Bearings calculations

Bearing	**A**	**B**
Vertical force	-136.174	1044

Horizontal force	-955.86	1088.26
Total radial force	965.5111071	1508.060286
Static load value	579.3066642	904.8361719
Static load value used for calculations	965.5111071	1508.060286
C0 (Static load rating)	1448.266661	2262.09043
Static load rating (kN) [C0]	1.448266661	2.26209043
Basic dynamic load rating (Ball bearing) (kN) [C]	2.022927149	3.159669603
Basic dynamic load rating (Roller bearing) (kN) [C]	0.980543967	1.531540554

The final bearings chosen were Deep Groove ball bearings.

Fixtures and Fittings

Table 6: Key sizing at each node

Node	2	4		5
Torque at position	-104.4	-104.4		208.8
Radius at position	0.013	0.021		0.0175
Force due to torque (Nm)	-8030.769231	-4971.4286		11931.4286
Minimum l_1 (mm)	15.20131536	9.41033808		22.5848114
Minimum l_2 (mm)	20.06053375	12.4184257		29.8042216
Constraints (mm)	L>10.52	L>9.66	L>23.67	
Design factor	6.12			
Allowable stress Sy/Ny	114379085			
Relevant SCF (K_b)	1.740394715	1.8531214		1.87941882
Relevant SCF (K_t)	1.445963885	1.47302005		1.79541024
Effective load on shaft due to key	89897687.02	22014686.6		80048594.3
OK?	78.5962635	19.247126		69.9853425

The table summarises that the key sizing and locations chosen were suitable and could handle the transmission loads.

Geometric features

The number of loading points and loading magnitudes in each section made finding the optimal diameters difficult. As seen in the figure below, a graph was made where the ideal diameter was plotted against the length along the shaft, considering the loads being applied. Despite the graph also producing accurate value representations for the shear force and bending moment diagrams and verifying our calculated loads, the graph plotted recommendations. This however doesn't mean the recommendations are practical as seen in section one where it advised a diameter ranging from 0mm to 2mm

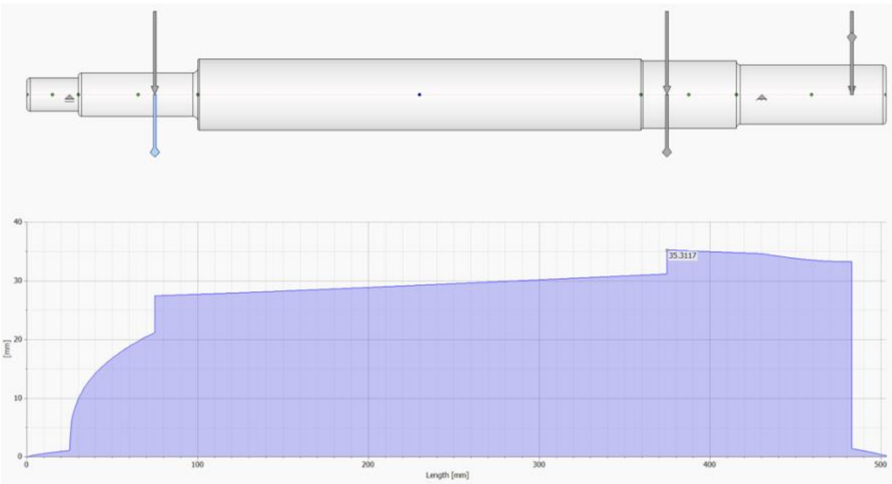

Figure 10 – Ideal diameters at different lengths along the shaft

The advice was taken from the graph for sections 2, 4 and 5 but not 1 and 3. Section 3 was required to be slightly larger than 2 and 4 to give the sprockets a shoulder for location. Section 1, practically speaking, cannot be a couple of millimetres thick as any vibrations induced would put the shaft at risk of breaking. A big step in diameter from section 2 to section 3 was chosen simply to reduce the weight. The stress concertation factor was reduced by using a fillet radius of 3mm. The shaft, when loaded, also produces a deflection. Maximum deflection is found in section 5 where the driven

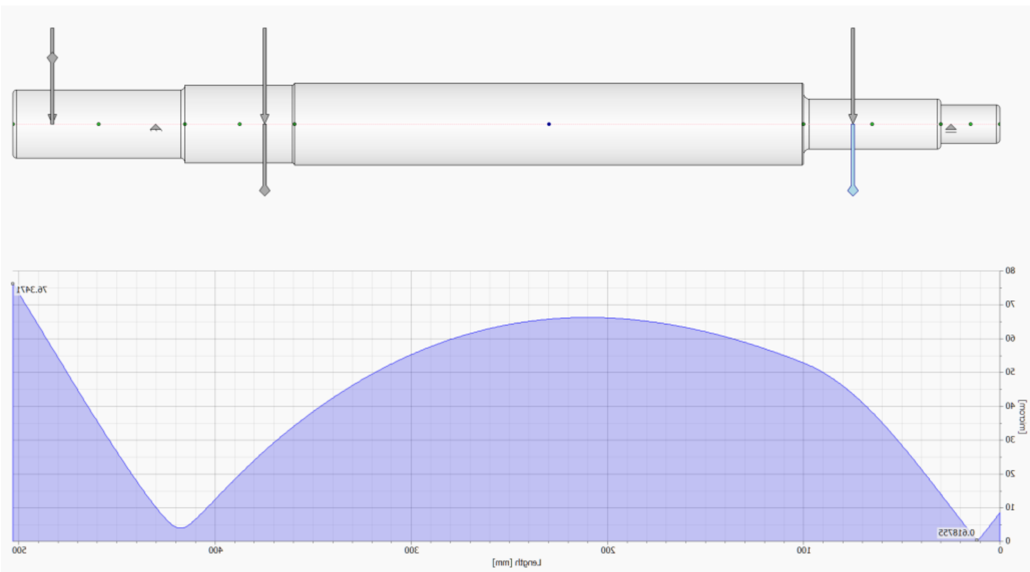
Figure 11 – Shaft deflection

sprocket is located with a deflection value of 76.35μm and an angle of 0.05 degrees. There is also a deflection at the centre of the shaft at section 3, albeit slightly less at 66.3μm with an angle of 0.0069 degrees. Despite the relatively large deflection in section 3, it is spread over a larger distance, which is why the angle of deflection is small. Due to this, we decided to neglect deflection in section 3 and only account for it in terms of diameter in section 5.

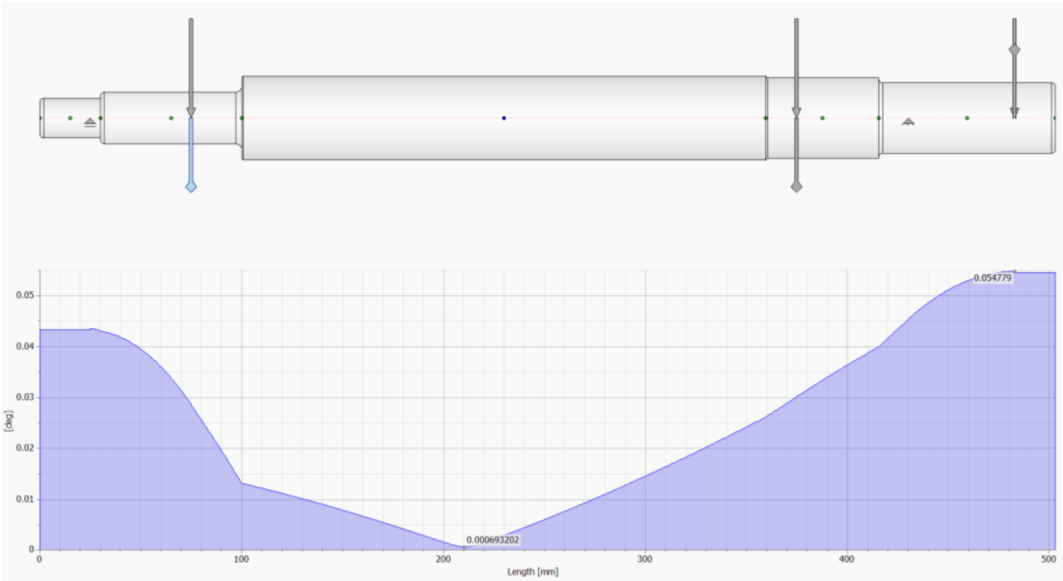

Figure 12 – Shaft deflection angle

Summary of fixtures and fittings:

Section 1 standard components: DIN 471 A20 retaining ring, 6204-RSH bearing [Thermal expansion allowed by float in bearing housing].
Section 2 standard components: 1210-26 Taper lock with 8x7x25 key.
Section 4 standard components: 2012-40 Taper lock with 12x8x25 key.
Section 5 standard components: 30mm bore SPEEDI SLEEVE, 2012-35 Taper lock with 10x8x30 key, 6008-RS1 bearing [Fully located by shaft shoulder and sleeve].

Conclusions

The driving sprocket should be as close to the supporting bearing as possible. To balance this and the functionality of maintenance, the sprocket was chosen to be on the outside. The geometric, and kinematic constraints and force requirements were all met. The sprocket is located outside the supporting bearing to make maintenance easier. EN24 medium low-alloy steel was chosen due to its high yield strength, allowing us to minimise shaft diameter. Compared to the sprocket being located inside, our design saw an increase of embodied carbon by 35.4% which was mainly due to the difference in billet sizing. Steels with lower embodied carbons were considered but resulted in larger diameters, increasing the initial billet size.

The bearings used are sealed, preventing lubrication from spilling, and protecting the interiors from contamination. The fixings remain secure due to appropriate tolerancing at each particular section where the standard component would be found. Keys were chosen over splines and a belt over a chain to reduce overall assembly cost and to make the design suitable for small batch production. The shaft is designed to allow all components to slide over each end of the shaft. Regular changes in diameters allow for weight reduction and for minimisation of tight, sliding parts.

The shaft could be improved in multiple ways:

1. The middle section of the shaft is cylindric but has no loads acting on it. Due to this, the middle section could be curved, reducing the weight of the shaft. This however increases the amount of material wasted per billet bought.
2. The forces acting on the shaft were assumed to have been point loads. For more accurate calculations, use Macauley's notation for loads acting over relative areas i.e., track force acts over 10mm sprocket hub.
3. Account for the weight of the final shaft in initial load calculations.

References

GD&T Lesson 5: Runout Tolerances. 2022. YouTube. Available from: https://www.youtube.com/watch?v=kiV-da6cli8 [Accessed 8 Nov. 2022].

Anon, n.d. [online] SMB Bearings. Available from: https://www.smbbearings.com/technical/bearing-tolerance-tables.html [Accessed 7 Nov. 2022].

Anon, n.d. *Tolerances for bearings seats and abutments*. [online] SKF. Available from: https://www.skf.com/uk/products/rolling-bearings/principles-of-rolling-bearing-selection/bearing-selection-process/bearing-interfaces/tolerances-for-bearing-seats-and-abutments [Accessed 8 Nov. 2022].

Anon, n.d. *ISO limits and fits*. [online] ISO Limits and Fits Table - The right fits and clearance for bearings and seals. Available from: https://simplybearings.co.uk/shop/Info-Pages-ISO-Limits/c4746_4779/index.html?page=1 [Accessed 10 Nov. 2022].

Anon, n.d. Available from: https://moodle.bath.ac.uk/pluginfile.php/1268086/mod_resource/content/1/SKF-rolling-bearings-catalogue.pdf.

Anon. *Transmission chain – installation, maintenance & designer guide.* Renold, 2017.

NC Bremer. Heavy duty chain drives for marine propulsion service. *Trans, of ASME,* 69:441-452, 1947.

Michael Clifford, Kathy Simmons, and Philip Shipway. *An introduction to mechanical engineering.* CRC Press, 2012.

H.B. Howard. The safety of structures. Sir Alfred Pugsley. Edwin Arnold, London. 1966. 156 pp. diagrams. 36s. *Journal of the Royal aeronautical society,* 71(675):227, mar 1967.

Edward Shigley Joseph, R Mischke Charles, and G Budynas Richard. Mechanical engineering design. *Mc Graw Hill, 2001.*

R.C. Juvinellan and H. Saunders. Fundamentals of machine component design. *Journal of Mechanisms Transmissions and Automation in Design,* 105(4):607, 1983.

Charles Lipson and Robert C Juvinall. *Handbook of stress and strength: design and material applications.* Macmillan, 1963.

S. Mahalingam. Polygonal action in chain drives. *Journal of the Franklin Institute,* 265(1):23-28,1958.

RA Morrsion. Polygonal action in chain drives. *Machine design,* 24(9): 155-159, 1952.

Gerhard Pahl and Wolfgang Beitz. *Engineering design: A systemic approach.* Springer Science & Business Media, 2013.

L Norton Robert. Machine design an intergrated approach. *Pearson Prentice Hall Publishers, USA, 2006.*

Anon, n.d. *PTI taper bushes*. [online] Available from: https://www.pti.eu/pdf/adapters/TaperBushes.pdf [Accessed 10 Nov. 2022].

Bonnett A. H., (1998). Cause, analysis and prevention of motor shaft failures. U.S. Electrical motors, Division of Emerson Electric, ST. Louis, Missouri, IEEE. 166-180.

Juvinall R. C; Marshek K. M (2008). Fundamentals of Machine component design. Fifth edition, John-Wiley and Sons.

Coimbatore, India.

Norton, R. L., (2006). Machine design: an integrated Approach. Third edition, Pearson Education, Upper Saddle River, NJ.

Pedersen, N. L., (2009). Stress concentrations in keyways and optimization of keyway design. Journal of Strain Analysis, 45, 593-604.

Pilkey, W. D. (1997). Peterson's stress concentration factors. Third edition, John-Wiley and Sons, New York.

Xiaobin Le P.E.; Mr. Zelong Le (2013). Stress concentration factors due to typical geometric discontinuities for shaft design by numerical simulation. American Society for Engineering Education, 120th ASEE Annual Conference & Exposition.

Appendix 1: Design Factor tables

Table 7: Values of X-Factors

Characteristic	B =	vg	g	f	p
	C =				
A = vg	vg	1.10	1.30	1.50	1.70
	g	1.20	1.45	1.70	1.95
	f	1.30	1.60	1.90	2.20
	p	1.40	1.75	2.10	2.45
A = g	vg	1.40	1.55	1.80	2.05
	g	1.45	1.75	2.05	2.35
	f	1.60	1.95	2.30	2.65
	p	1.75	2.15	2.55	2.95
A = f	vg	1.50	1.80	2.10	2.40
	g	1.70	2.05	2.40	2.75
	f	1.90	2.30	2.70	3.10
	p	2.10	2.55	3.00	3.45
A = p	vg	1.70	2.15	2.40	2.75
	g	1.95	2.35	2.75	3.15
	f	2.20	2.65	3.10	3.55
	p	2.45	2.95	3.45	3.95

vg = very good, g = good, f = fair, p =poor

Table 8: Value of Y-Factors

Characteristic D =	Not serious	Serious	Very serious
E= not serious	1.0	1.2	1.4
E = Serious	1.1	1.3	1.5
E = Very serious	1.2	1.4	1.6

Appendix 2: Calculations for driving the sprocket inside the bearing

Table 10: Calculations for driving sprocket inside the bearing

Node	**1**	**2**	**3**	**4**	**5**
Diameter, d (m)	0.024	0.03	0.036	0.04	0.035
Length of node	0.005	0.07	0.29	0.07	0.005
J value	3.2572E-08	7.95216E-08	1.64896E-07	2.51327E-07	1.47324E-07
I value	1.6286E-08	3.97608E-08	8.2448E-08	1.25664E-07	7.36618E-08
Vertical BM	0	-1.815652	-29.050432	-32.681736	2.13163E-13
Horizontal BM	0	13.4152	-1.3568	-32.1264	2.41585E-13
Combined BM	0	13.53751023	29.0820994	45.82795484	3.22182E-13
Torque	0	-104.4	-104.4	208.8	0
Bending SCF	1.780867465	1.886402586	1.977257105	2.031742088	1.962938327
Torsional SCF	1.424781117	1.495136051	1.555191459	1.590990112	1.545756993
Nominal Bending stress	0	5107109.144	6349190.501	7293745.545	7.65416E-08
Max bending stress	0	9634063.899	12553982.03	14819009.8	1.50247E-07
Nominal Torsional stress	0	-19692771.63	-11396279.88	16615776.06	0
Max torsional stress	0	-29443372.8	-17723397.13	26435535.41	0
Combined stresses	0	51899439.23	33165628.02	48126039.2	1.50247E-07
Allowable stress	85784313.73	85784313.73	85784313.73	85784313.73	85784313.73

OK?	0	60.49991773	38.66164638	56.10121141	1.75145E-13

Table 11: Resultant Calculations

Total mass (KG)	4.04473394
Embodied CO2 (KG)	8.089467879
Total cost (£)	**WILL BE WORKED OUT TOMORROW**

Table 12: Steel type properties for reference

Material	**Strength (Pa)**	**Density (kg/m3)**	**Allowable stress**
EN3A 070M20 - General purpose mild steel	215000000	7900	35130718.95
EN8 080M40 - Carbon manganese steel	280000000	7900	45751633.99
EN16 605M36 - Low alloy manganese-molybdenum steel	525000000	7900	85784313.73
EN24 817M40 - Medium carbon low alloy steel	680000000	7900	111111111.1

Table 13: Bending SCF diameter ratio

Bending		
D/d	**B**	**a**
1.3	0.938	-0.258
1.615384615	0.893	-0.309
0	0.938	-0.258
1.05	0.951	-0.238
1.142857143	0.951	-0.238

Table 14: Torsional SCF diameter ratio

Torsional		
D/d	**B**	**a**
1.3	0.863	-0.239
1.615384615	0.863	-0.239
0	0.833	-0.216
1.05	0.833	-0.216
1.142857143	0.833	-0.216

Table 15: Bending SCF from chart, for reference

Bending SCF – chart		
D/d	**B**	**a**
6	0.879	-0.332
3	0.893	-0.309
1.5	0.938	-0.258
1.1	0.951	-0.238
1.03	0.981	-0.184

1.01	0.919	-0.17

Table 16: Torsional SCF from chart, for reference

Torsional SCF from chart		
D/d	**B**	**a**
2	0.863	-0.239
1.2	0.833	-0.216
1.09	0.903	-0.127

Appendix 3: Calculations for a chain drive

Following Fenner chain selection process

1. Service factor = 1.1
2. Design power = 2.2kW
3. Driving pulley: 3000 rpm
   Driven pulley: 916 rpm
   Here the calculation stopped as there was not a suitable Fenner chain for these specifications

Following the Renolds chain selection process
Note: a centre distance of 415-450 was required, for calculations an assumed centre distance of 420mm was chosen

1. z_1= 19
   A speed ratio of 3.275 subsequently gave z_2= 57

2. f_1= 1.5, as z_1= 19, f_2 = 1
3. $selection\ power = p\ x\ f_1\ x\ f_2 = 30kW$

Here, when referenced to the chart Renolds chart, a 15.875mm pitch chain could be selected for a 19T duplex chain. It can be seen that it is immediately on the edge of acceptability. At this point it was decided to choose a belt drive.

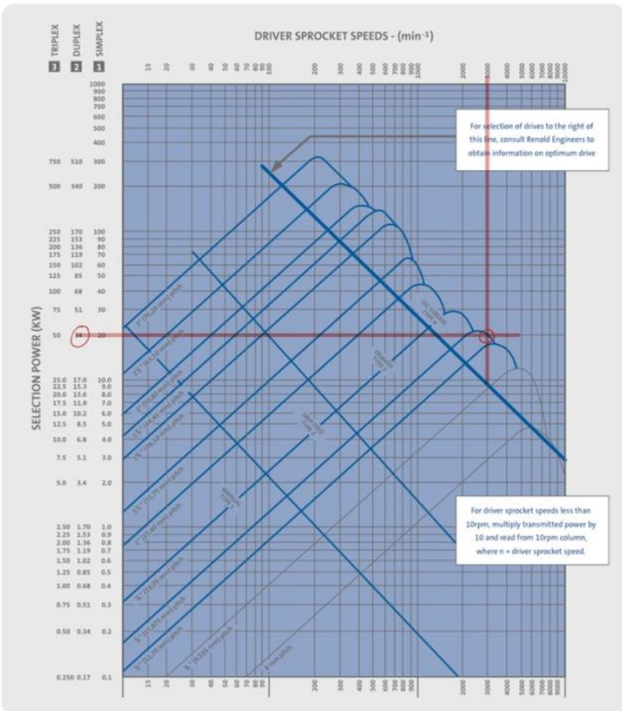

Figure 13: Renold Chain designer guide

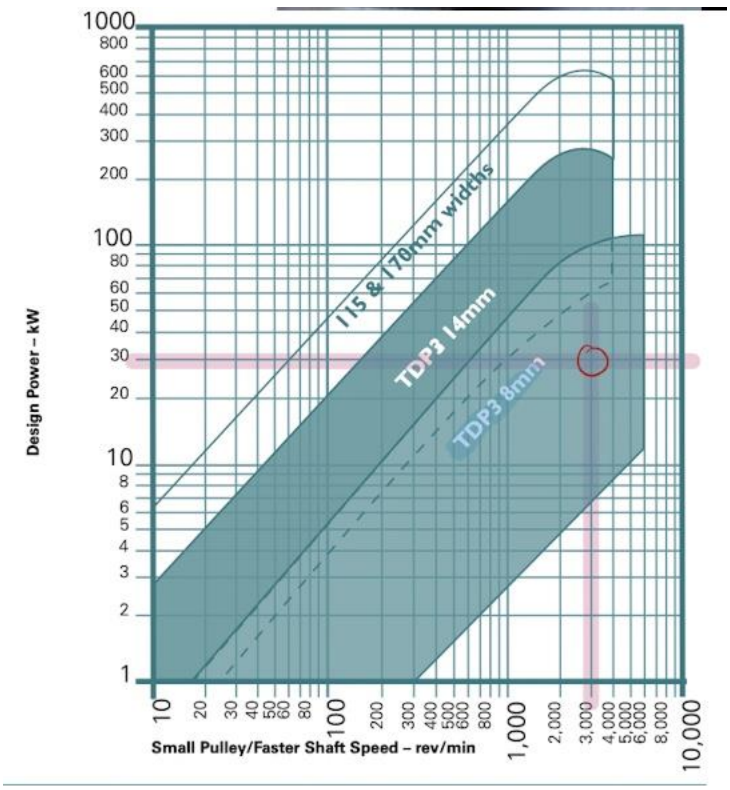

Figure 14: Fenner Belt Pitch Selection guide

CENTRE DISTANCE IN MILLIMETRES

Speed Ratio	Number of grooves on Driving Pulley	Number of grooves on Driven Pulley	Belt pitch length in millimetres 480	560	600	640	720	800	880	960	1040	1120	1200	1280	1440	1600	1760	1800	2000	2400	2600	2800	Speed Ratio
			60 teeth	70 teeth	75 teeth	80 teeth	90 teeth	100 teeth	110 teeth	120 teeth	130 teeth	140 teeth	150 teeth	160 teeth	180 teeth	200 teeth	220 teeth	225 teeth	250 teeth	300 teeth	325 teeth	350 teeth	
2.50	32	80	–	–	–	–	–	165	207	248	290	330	371	411	492	573	653	673	774	974	1074	1174	2.50
2.50	36	90	–	–	–	–	–	–	–	217	259	300	341	382	463	544	624	644	745	946	1046	1146	2.50
2.55	44	112	–	–	–	–	–	–	–	–	–	232	274	316	399	480	561	582	683	884	984	1085	2.55
2.57	28	72	–	–	–	–	150	192	233	274	315	356	396	436	517	597	678	698	798	998	1099	1199	2.57
2.57	56	144	–	–	–	–	–	–	–	–	–	–	–	–	299	384	467	487	589	792	893	994	2.57
2.63	64	168	–	–	–	–	–	–	–	–	–	–	–	–	–	–	394	415	519	724	825	927	2.63
2.65	34	90	–	–	–	–	–	–	178	220	262	304	345	385	467	547	628	648	749	949	1050	1150	2.65
2.67	24	64	–	–	–	134	177	218	259	300	340	381	421	461	542	622	702	722	822	1023	1123	1223	2.65
2.67	30	80	–	–	–	–	–	168	210	252	293	334	375	415	496	576	657	677	777	978	1078	1178	2.67
2.67	72	192	–	–	–	–	–	–	–	–	–	–	–	–	–	–	–	–	446	654	757	858	2.67
2.77	26	72	–	–	–	–	153	195	237	278	319	359	400	440	521	601	681	702	802	1002	1102	1203	2.77
2.80	40	112	–	–	–	–	–	–	–	–	–	238	281	323	406	487	569	589	690	891	992	1092	2.80
2.81	32	90	–	–	–	–	–	–	181	224	266	307	348	389	470	551	632	652	752	953	1053	1154	2.81
2.86	28	80	–	–	–	–	–	171	214	255	297	338	378	419	500	580	661	681	781	982	1082	1182	2.86
2.95	38	112	–	–	–	–	–	–	–	–	–	242	284	326	409	491	572	593	694	895	996	1096	2.95
3.00	24	72	–	–	–	–	156	199	240	281	322	363	403	444	524	605	685	705	806	1006	1106	1206	3.00
3.00	30	90	–	–	–	–	–	–	184	227	269	311	352	393	474	555	635	656	756	957	1057	1157	3.00
3.00	48	144	–	–	–	–	–	–	–	–	–	–	–	–	312	397	480	501	604	807	908	1009	3.00
3.00	56	168	–	–	–	–	–	–	–	–	–	–	–	–	–	320	407	428	533	738	840	941	3.00
3.00	64	192	–	–	–	–	–	–	–	–	–	–	–	–	–	–	–	350	459	668	771	873	3.00
3.08	26	80	–	–	–	–	–	174	217	259	300	341	382	422	503	584	664	685	785	986	1086	1186	3.08
3.11	36	112	–	–	–	–	–	–	–	–	–	245	288	330	413	495	576	596	697	899	999	1100	3.11
3.21	28	90	–	–	–	–	–	–	187	230	273	314	355	396	477	558	639	659	760	961	1061	1161	3.21
3.27	44	144	–	–	–	–	–	–	–	–	–	–	–	–	319	404	487	508	611	814	915	1016	3.27
3.29	34	112	–	–	–	–	–	–	–	–	204	248	291	333	416	498	579	600	701	903	1003	1104	3.29
3.33	24	80	–	–	–	–	–	178	220	262	304	345	385	426	507	588	668	688	789	989	1090	1190	3.33
3.43	56	192	–	–	–	–	–	–	–	–	–	–	–	–	–	–	340	363	472	682	785	887	3.43
3.46	26	90	–	–	–	–	–	–	191	234	276	318	359	400	481	562	643	663	764	985	1065	1165	3.46
3.50	32	112	–	–	–	–	–	–	–	–	207	251	294	337	420	502	583	603	705	906	1007	1107	3.50
3.50	48	168	–	–	–	–	–	–	–	–	–	–	–	–	–	333	420	442	547	752	854	956	3.50
3.60	40	144	–	–	–	–	–	–	–	–	–	–	–	–	325	411	494	515	618	821	922	1023	3.60
3.73	30	112	–	–	–	–	–	–	–	–	210	255	298	340	423	505	587	607	708	910	1011	1111	3.73
3.75	24	90	–	–	–	–	–	–	194	237	279	321	362	403	485	566	647	667	767	968	1069	1169	3.75
3.79	38	144	–	–	–	–	–	–	–	–	–	–	–	–	328	414	498	518	621	825	926	1027	3.79
3.82	44	168	–	–	–	–	–	–	–	–	–	–	–	–	–	339	427	448	553	760	862	963	3.82
4.00	28	112	–	–	–	–	–	–	–	–	213	258	301	343	427	509	590	611	712	914	1014	1115	4.00
4.00	36	144	–	–	–	–	–	–	–	–	–	–	–	–	331	417	501	522	625	829	930	1031	4.00
4.00	48	192	–	–	–	–	–	–	–	–	–	–	–	–	–	–	352	375	485	696	799	901	4.00
4.20	40	168	–	–	–	–	–	–	–	–	–	–	–	–	–	346	433	455	560	767	869	970	4.20
4.24	34	144	–	–	–	–	–	–	–	–	–	–	–	244	335	421	505	525	628	832	933	1035	4.24
4.31	26	112	–	–	–	–	–	–	–	–	216	261	304	347	430	512	594	614	716	917	1018	1119	4.31
4.36	44	192	–	–	–	–	–	–	–	–	–	–	–	–	–	–	358	381	492	703	806	908	4.36
4.42	38	168	–	–	–	–	–	–	–	–	–	–	–	–	–	349	437	459	564	770	872	974	4.42
4.50	32	144	–	–	–	–	–	–	–	–	–	–	–	247	338	424	508	529	632	836	937	1038	4.50
4.67	24	112	–	–	–	–	–	–	–	–	219	264	308	350	434	516	597	618	719	921	1022	1122	4.67
4.67	36	168	–	–	–	–	–	–	–	–	–	–	–	–	–	352	440	461	567	774	876	978	4.67
4.80	30	144	–	–	–	–	–	–	–	–	–	–	–	250	341	427	511	532	635	839	941	1042	4.80
4.80	40	192	–	–	–	–	–	–	–	–	–	–	–	–	–	–	365	388	498	710	813	916	4.90
4.94	34	168	–	–	–	–	–	–	–	–	–	–	–	–	–	355	443	465	570	777	879	981	4.94
5.05	38	192	–	–	–	–	–	–	–	–	–	–	–	–	–	–	368	391	502	713	816	919	5.05
5.14	28	144	–	–	–	–	–	–	–	–	–	–	–	253	344	431	515	536	639	843	944	1046	5.14
5.25	32	168	–	–	–	–	–	–	–	–	–	–	–	–	–	358	446	468	574	781	883	995	5.25
5.33	36	192	–	–	–	–	–	–	–	–	–	–	–	–	–	–	371	394	505	716	820	923	5.33
5.54	26	144	–	–	–	–	–	–	–	–	–	–	–	256	348	434	518	539	642	847	948	1049	5.54
5.60	30	168	–	–	–	–	–	–	–	–	–	–	–	–	–	361	450	471	577	784	887	988	5.60
5.65	34	192	–	–	–	=	–	–	–	–	–	–	–	–	–	–	374	397	508	720	823	926	5.65
6.00	24	144	–	–	–	–	–	–	–	–	–	–	–	259	351	437	522	542	646	850	952	1053	6.00
6.00	28	168	–	–	–	–	–	–	–	–	–	–	–	–	269	364	453	475	581	785	890	992	6.00
6.00	32	192	–	–	–	–	–	–	–	–	–	–	–	–	–	–	377	400	511	723	827	930	6.00
6.40	30	192	–	–	–	–	–	–	–	–	–	–	–	–	–	–	380	403	515	727	830	933	6.40
6.46	26	168	–	–	–	–	–	–	–	–	–	–	–	–	272	368	478	456	584	791	894	996	6.46
6.86	28	192	–	–	–	–	–	–	–	–	–	–	–	–	–	–	383	406	519	730	834	937	6.86

All centre distances are rounded values – Consult your local Authorised Distributor if centre distance is fixed.

Figure 3: demonstrates the belt pitch length selection process